Journal of Hydrology 375 (2009) 312–325

Contents lists available at ScienceDirect

Journal of Hydrology

journal homepage: www.elsevier.com/locate/jhydrol

Controls on event runoff coefficients in the eastern Italian Alps

Daniele Norbiato [a,*], Marco Borga [a], Ralf Merz [b], Günther Blöschl [b], Alberto Carton [c]

[a] Department of Land and Agroforest Environments, University of Padova, AGRIPOLIS, viale dell'Universita, 16, IT-35020 Legnaro, Italy
[b] Technical University of Wien, Wien, Austria
[c] Department of Geography, University of Padova, Italy

ARTICLE INFO

Article history:
Received 14 March 2008
Received in revised form 14 May 2009
Accepted 16 June 2009

This manuscript was handled by K. Georgakakos, Editor-in-Chief, with the assistance of Christa D. Peters-Lidard, Associate Editor

Keywords:
Event runoff coefficient
Runoff generation
Geology
Soil moisture initial conditions

SUMMARY

Analyses of event runoff coefficients provide essential insight on catchment response, particularly if a range of catchments and a range of events are compared by a single indicator. In this study we examine the effect of climate, geology, land use, flood types and initial soil moisture conditions on the distribution functions of the event runoff coefficients for a set of 14 mountainous catchments located in the eastern Italian Alps, ranging in size from 7.3 to 608.4 km^2. Runoff coefficients were computed from hourly precipitation, runoff data and estimates of snowmelt. A total of 535 events were analysed over the period 1989–2004. We classified each basin using a "permeability index" which was inferred from a geologic map and ranged from "low" to "high permeability". A continuous soil moisture accounting model was applied to each catchment to classify 'wet' and 'dry' initial soil moisture conditions. The results indicate that the spatial distribution of runoff coefficients is highly correlated with mean annual precipitation, with the mean runoff coefficient increasing with mean annual precipitation. Geology, through the 'permeability index', is another important control on runoff coefficients for catchments with mean annual precipitation less than 1200 mm. Land use, as indexed by the SCS curve number, influences runoff coefficient distribution to a lesser degree. An analysis of the runoff coefficients by flood type indicates that runoff coefficients increase with event snowmelt. Results show that there exists an intermediate region of subsurface water storage capacity, as indexed by a flow–duration curve-based index, which maximises the impact of initial wetness conditions on the runoff coefficient. This means that the difference between runoff coefficients characterised by wet and dry initial conditions is negligible both for basins with very large storage capacity and for basins with small storage capacity. For basins with intermediate storage capacities, the impact of the initial wetness conditions may be relatively large.

Introduction

Predicting flood response in ungauged catchments is emerging as one of the major issues in the hydrological science (Sivapalan et al., 2003). Predictions are particularly difficult to make in alpine regions where data are sparse and the spatial variability of both precipitation and physical controls on runoff generation is huge. The event runoff coefficient, defined as the portion of rainfall that becomes direct runoff during an event, is a key concept in hydrology and an important diagnostic variable for catchment response, particularly if a range of catchments and a range of events are to be compared by a single indicator (Merz and Blöschl, 2009). Analysis of event runoff coefficients may provide essential insight on how different landscapes 'filter' rainfall to generate runoff and how the observed differences can be explained by catchment characteristics (Blume et al., 2007). Quantifying process controls on space and time variability of runoff coefficients may therefore contribute to isolate flood-generating mechanisms both in time (summer vs. winter, rainfall vs. snowmelt, etc.), and also in space (different climate, geology, soils, vegetation, etc.) (Fiorentino and Iacobellis, 2001).

There exists a substantial body of work on controls of runoff coefficient variability at the regional scale (Merz and Blöschl, 2003). The scale dependency of runoff coefficients to plot and catchment area has been examined by Wainwright and Parsons (2002) and Cerdan et al. (2004), who both identified a significant decrease in the runoff coefficient as area increases. Furthermore, Cerdan et al. (2004) was able to show that at the scale of 10 km^2 the percentage of arable land is a driving factor for runoff response. Gottschalk and Weingartner (1998) examined runoff coefficients for 192 flood events in 17 Swiss catchments, which they used in a derived flood frequency model. They fitted a Beta function to the distribution of runoff coefficients in each catchment and interpreted the parameters for different hydrologic regions in Switzerland. They concluded that the differences in runoff coefficients can be explained by topographic characteristics such as altitude and slope and to some degree by stream network density and

* Corresponding author. Tel.: +39 049 8272681; fax: +39 049 8272686.
E-mail address: daniele.norbiato@unipd.it (D. Norbiato).

0022-1694/$ - see front matter
doi:10.1016/j.jhydrol.2009.06.044

geology. A larger flood events data set was examined by Merz and Blöschl (2009), who analysed a total of about 50,000 events in 337 Austrian catchments with catchment areas ranging from 80 to 10,000 km^2 over the period 1981–2000. They found that, in the type of climate and at the scale of the catchments examined in their work, the main controls on event runoff coefficients were the climate and the runoff regime through the seasonal catchment water balance and hence antecedent soil moisture conditions in addition to event characteristics. Catchment characteristics such as soils, land use and geology affected runoff coefficients to a lesser degree.

In this paper, we characterise the distribution of event runoff coefficients for 14 catchments in the eastern Italian Alps. The size of the catchments ranges from 7.3 to 608.4 km^2. In this region, interaction of orographic structure with large scale atmospheric patterns results in large spatial variability in the precipitation and flood regime, and translates into marked differences of the distribution of event runoff coefficients. There is, however, considerable spatial variability in the degree to which runoff coefficients reflects the precipitation pattern. Specifically, we address the following research questions: (a) What are the main controls on the spatial variability of event runoff coefficients? (b) How variability in climate, geology and land use can be related to spatial differences in runoff coefficient distributions? (c) How is the influence of antecedent soil moisture conditions filtered by geo-hydrologic characteristics of the catchments?

In particular we characterise the distribution of runoff coefficients with respect to a broad geologic partitioning of the region according to the permeability characteristics of the lithological units, as inferred from geological surveys. A number of studies identified low correlation between geological indices and the distribution of event runoff coefficients (Merz and Blöschl, 2009 and references therein). A possible reason for the apparent low predictive power of geological indices may be the use of the percentage of catchment area covered by a given geological unit to characterise the process controls on the runoff coefficients. Although this is the type of information typically available for practical applications, it seems not to be representative as even within the same geological unit, the runoff generation can differ vastly, depending on preferential flow through fissures and fractures, as illustrated by many case studies around the world. (Tague and Grant, 2004). Conceptually, our approach follows Winter (2001) and Tague and Grant (2004), who advocate hydrologic comparison based on geologic–geomorphic landscape attributes. We classified each basin using a "permeability index" which ranges from "low" to "high permeability". The classification metric incorporates information on the inferred degree of secondary permeability (i.e. the permeability effects developed in a rock after its deposition, through weathering and fracturing) and on the spatial organisation of the lithological unit with respect to the river network. The lateral contiguity of distinct lithological units provides a unique opportunity to examine geological control on runoff coefficients distributions at the regional scale. Moreover, the geologic partitioning affords characterisation of the impact of initial moisture conditions on runoff coefficients for various permeability classes. To this purpose, a continuous soil moisture accounting model is applied to each catchment to derive soil moisture conditions prior to each event.

The paper is organised as follows. The Section "Study catchments: morphology, climate, land use and geology" describes the study area and the main attributes of catchments according to morphology, climate, land use and geology. The Section "Computation of event runoff coefficients" describes the technique used to estimate the event runoff coefficients, and specifically the baseflow separation method, the event separation method, the estimation of the runoff coefficient and the continuous soil moisture accounting model used to evaluate the initial soil moisture conditions. The analysis of the main controls on the runoff coefficient distributions is reported in the Section 'Results', with focus on the role of climate, geology, land use and initial soil moisture conditions. Finally, the overview of the principal observations from this work is presented in the Section "Conclusions".

Study catchments: morphology, climate, land use and geology

The location of the 14 catchments used in this study is shown in Fig. 1. Table 1 provides more detailed catchment information. For the sake of clarity, catchments are sequentially numbered as indicated in Table 1. Catchment drainage area ranges between 7.3 km^2 and 608.4 km^2. The topography is rather complex with altitudes ranging from 388 m asl (lowest altitude of Posina) to 3600 m asl (highest elevation of Ridanna at Vipiteno). Measured runoff represents the natural runoff variability well, since management activities, such as artificial reservoirs and diversions, do not alter the river regime. Five catchments are included in four larger parent basins (catchments 1 and 3 are included in catchment 2; catchments 5, 9 and 14 are included in catchments 4, 10 and 13, respectively).

Examination of Table 1 shows that these catchments exhibit significant variability in terms of hydrological response. A parameter which describes this variability is the ratio between the mean of maximum annual flood and the average annual discharge. Table 1 shows that catchments with similar drainage area, such as catchment 5 (San Vigilio at Longega), catchment 12 (Posina at Stancari) and catchment 13 (Cordevole at Saviner) (with areas ranging from 105.5 to 116.0 km^2) are characterised by values of the ratio ranging over more than one order of magnitude (from 2.4 to 33.2). This variability implies that different processes are responsible for flood runoff generation across these catchments. Qualitative information gathered during site visits was used to make educated guesses about the hydrological processes driving runoff generation during flood events. According to this information, for example, the response of the Posina catchment is dominated by quick subsurface flow and surface runoff generated on saturated areas, whereas the response of the San Vigilio catchment is delayed and attenuated due to large groundwater storage.

Estimates of catchment-averaged mean annual precipitation (MAP) reported in Table 1 were obtained by the Thiessen technique. The gauge densities range from 1 station per 4 km^2 (catchment 14 – Cordevole at Vizza) to 1 station per 150 km^2 (catchment 1 – Aurino at Cadipietra). Corrections for snowfall catch deficit (Sevruk et al., 1998) were used. Catchment-averaged mean annual precipitation ranges from 900 mm to 1708 mm. Precipitation is larger for the catchment located in the forealpine regions (catchment 12) and for some of the catchments most exposed to the *stau* effect (catchments 3 and 10). It is intermediate for the catchments located in the Dolomite region exposed to humid and warm winds from the Adriatic sea (catchments 13 and 14) and for the other catchments exposed to the *stau* effect (catchments 1, 2, 9 and 11). Precipitation is significantly lower in the catchments of Val Pusteria (catchments 4–8), due to the dual sheltering effect of the mountainous ranges to both the north and the south.

We applied the Budyko's climatic classification scheme (Budyko, 1974) to display the climatic characteristics of these catchments. This is achieved by presenting the specific response of each catchment on the Budyko curve (Fig. 2), which is a plot that expresses E/P, the ratio of average annual evapotranspiration (E) to average annual precipitation (P) as a function of EP/P, the ratio of average annual potential evapotranspiration (EP) to average annual precipitation (P). Actual evapotranspiration (E) for each catchment was derived as the long-term difference between P and R (runoff) for the basins, whereas potential evapotranspiration was

Catchment number	Station name
1	Aurino at Cadipietra
2	Aurino at San Giorgio
3	Riva at Seghe
4	Gadera at Mantana
5	San Vigilio at Longega
6	Casies at Colle
7	Rienza at Monguelfo
8	Anterselva at Bagni
9	Plan at Plan
10	Passirio at Saltusio
11	Ridanna at Vipiteno
12	Posina at Stancari
13	Cordevole at Saviner
14	Cordevole at Vizza

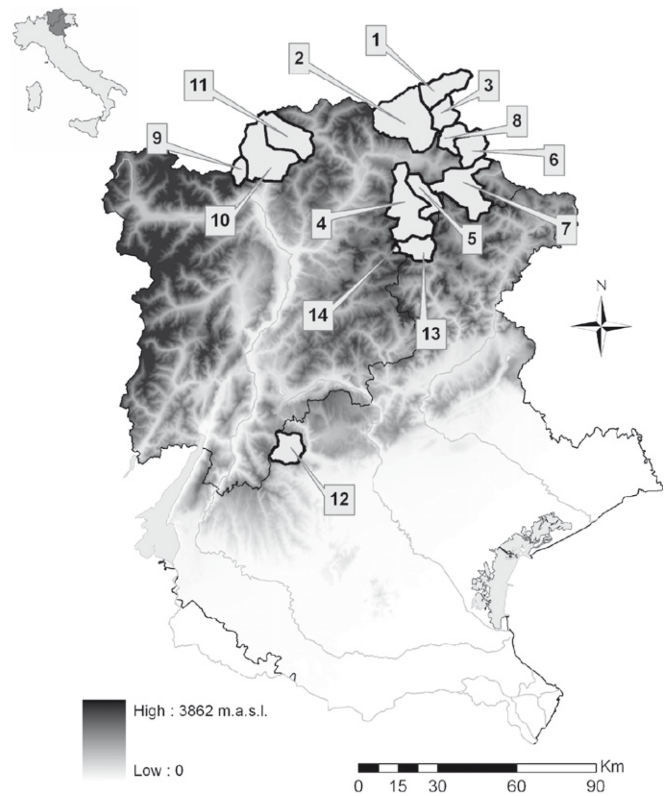

Fig. 1. Study catchments and their location in Italy.

Table 1
Catchments characteristics.

Catchment number	Station name	Area (km^2)	Elevation range (m asl)	Mean annual precipitation (mm)	Mean annual runoff (mm)	Annual runoff ratios	Mean maximum annual flood (m^3/s)	Mean maximum annual flood/mean discharge
1	Aurino at Cadipietra	149.8	1035–3400	1520	1276	0.84	40.3	6.7
2	Aurino at San Giorgio	608.4	816–3400	1351	1033	0.76	136.4	6.6
3	Riva at Seghe	91.4	1520–3400	1659	1283	0.77	36.5	9.7
4	Gadera at Mantana	396.7	814–3200	963	623	0.65	62.0	7.9
5	San Vigilio at Longega	105.5	1010–3000	900	560	0.62	4.6	2.4
6	Casies at Colle	117.4	1196–2800	993	669	0.67	15.8	6.2
7	Rienza at Monguelfo	268.6	1096–3200	980	621	0.63	20.1	3.7
8	Anterselva at Bagni	82.4	1091–3200	1050	780	0.74	12.6	6.2
9	Plan at Plan	49.0	1575–3200	1520	1255	0.83	26.2	8.9
10	Passirio at Saltusio	342.4	442–3400	1580	1238	0.78	202.1	14.9
11	Ridanna at Vipiteno	210.2	940–3600	1375	1019	0.74	79.6	11.6
12	Posina at Stancari	116.0	388–2300	1708	1000	0.59	111.4	33.2
13	Cordevole at Saviner	109.0	1025–3200	1120	770	0.69	30.7	11.4
14	Cordevole at Vizza	7.3	1810–3200	1218	866	0.71	2.6	12.5

computed based on the Hargreaves method (Hargreaves and Samani, 1982). Fig. 2 shows clearly that all the basins are characterised by a wet climate and that the ratio of evapotranspiration to precipitation is controlled generally by catchment elevation (Table 1). This control is reflected in the pattern of mean annual runoff ratios, which range from 0.59 (catchment 12, Posina) to 0.84 (catchment 1, Aurino at Cadipietra).

Fig. 3 shows the mean monthly values of liquid precipitation, solid precipitation and runoff related to their mean annual values. All the alpine catchments are characterised by peaks of precipitation and runoff in the summer months. Catchment 12 (Posina at Stancari) shows two maximum values of mean monthly rainfall, the most important in autumn and the minor one during spring. The significance of snowfall implies that both the seasonal hydrological balance and the flood regime in these catchments are influenced by snow accumulation and melt.

Grassland, sparsely vegetated area (including outcrop rocks), coniferous and mixed forests are the most important types of land use in these catchments (Table 2). Outcrop rocks cover a considerable portion of Cachments 4 (Gadera at Mantana), 5 (San Vigilio at Longega) and 7 (Rienza at Monguelfo) and are strongly influenced by secondary permeability effects. The most significant glaciated area (6%) is located in catchment 9 (Plan at Plan) while catchment 12 (Posina at Stancari) is characterised by a heavily forested area (74%). Sparsely vegetated area dominates in catchment 3 (Riva at Seghe) (61%).

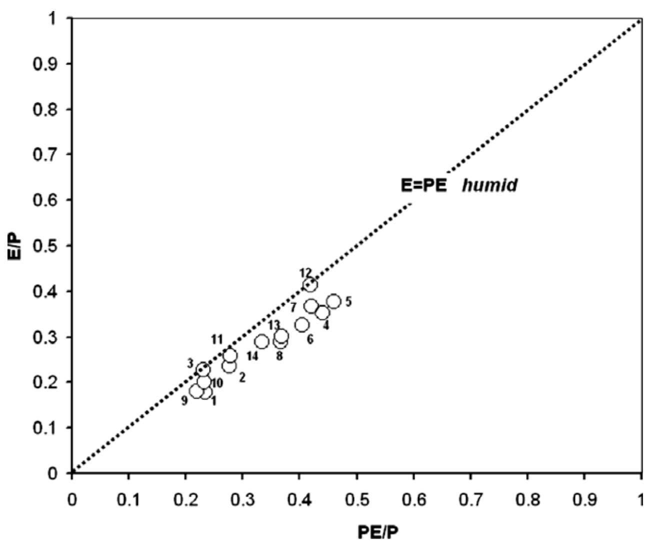

Fig. 2. Plot of mass balance data from the study basins on the Budyko curve.

For the purposes of this study, we classified the study catchments according to the permeability of the prevailing lithological units, using the 1:100,000 scale geologic map of Italy. Metamorphic and sedimentary rock units prevail across the study catchments. Igneous rocks, mainly represented by dykes intruding sedimentary rocks and/or scanty levels of tonalites within metamorphic rocks, are relatively rare. The most common metamorphic rocks cropping out in the study catchments are gneiss (in the varieties of orthogneiss and paragneiss), phyllites and micaschists. These rock types are characterised by a low to very low permeability and prevail in catchments 1, 2, 3, 6, and 8 to 11. In catchment 6, the arrangement of the rock types, which are symmetrical and orthogonal with respect to the river network, together with the secondary permeability due to fractures (milonite facies) considerably change the low permeability typical of metamorphic rocks; similarly, the permeability increases due to structures transverse to the flow lines in catchment 8.

Sedimentary rocks prevail in catchments 13 and 14, and belong to the typical Permian–Triassic dolomite series. These include a wide range of rock types: dolostones, bedded limestones, sandstones, conglomerates, pyroclastic products, sequences of carbonate–terrigenous deposits and evaporitic rocks. These units are characterised by a medium permeability. Sedimentary rocks found in catchment 12 are saccharoidal, stratified or massif dolostones with scanty strips of grey limestones with marly and clayey levels. When they are not subject to karst processes or fractured (which are present in a subbasin of this catchment), these rock types show a low to medium permeability.

Both metamorphic and carbonate rocks are present in catchments 4, 5 and 7, where significant karst processes are found, implying high permeability (Van de Griend et al., 1986).

Based on these analyses, a 'permeability index' has been derived for each catchment. The index summarises in a qualitative ranking the permeability characteristics and ranges from 1 to 3, representing conditions of low, intermediate and high permeability, respectively (Table 3). The derivation of the index has been based on (i) the percent coverage of each geologic formation; (ii) the influence of secondary permeability effects, inferred from tracers experiments (van de Griend et al., 1986) and local knowledge, and (iii) the position and orientation of each lithologic unit with respect to the river network.

Computation of event runoff coefficients

Runoff coefficients were computed over the period ranging from 1989 to 2004. The length of the hourly records of streamflow,

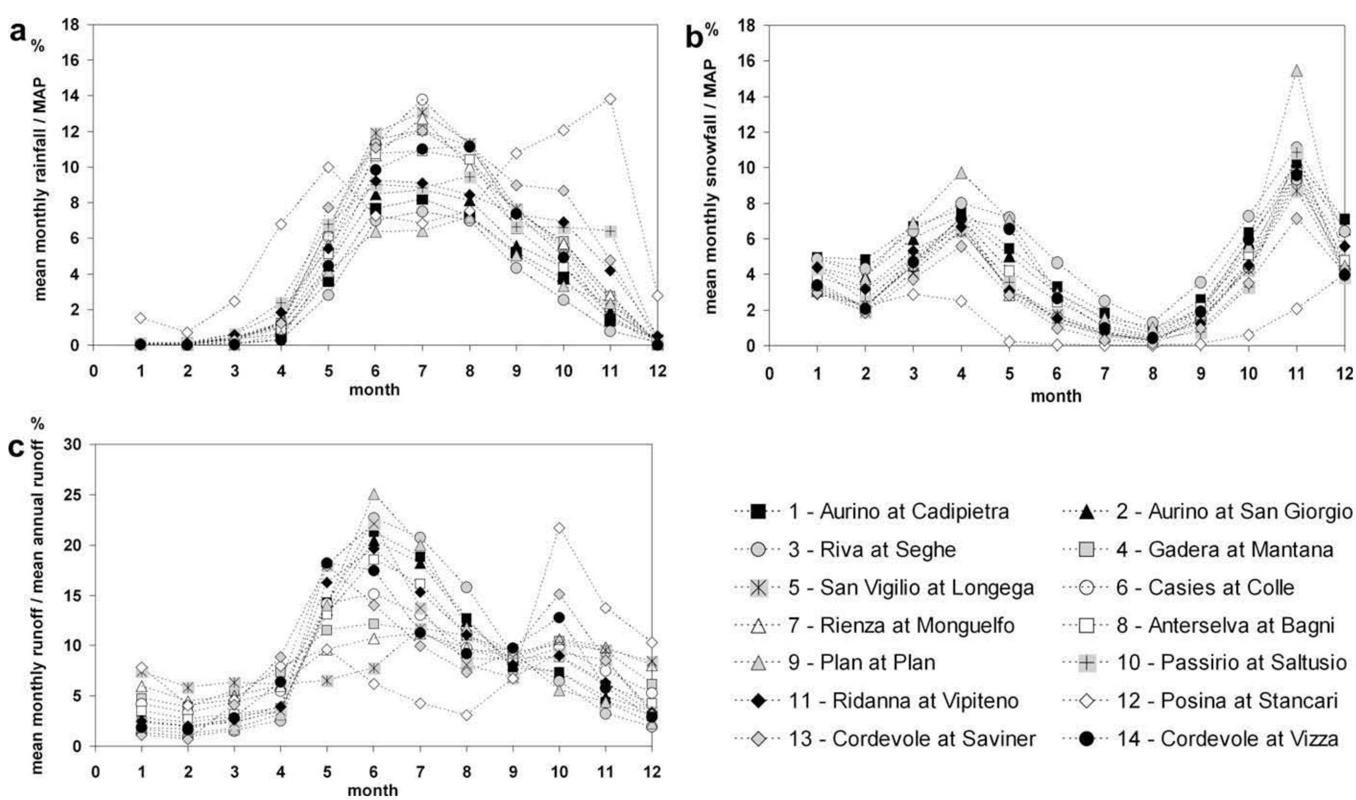

Fig. 3. (a) Mean monthly rainfall over MAP, (b) mean monthly snowfall over MAP and (c) mean monthly runoff over mean annual runoff.

Table 2
Land use for the study catchments.

Catchment number	Station name	Discontinuos urban fabric (%)	Arable land (%)	Grassland (%)	Coniferous forest (%)	Broad leaved and mixed forest (%)	Glaciers (%)	Sparsely vegetated areas (%)
1	Aurino at Cadipietra	0	0	36	22	1	3	38
2	Aurino at San Giorgio	0	1	30	30	3	4	32
3	Riva at Seghe	0	0	26	12	1	0	61
4	Gadera at Mantana	1	0	26	41	8	0	24
5	San Vigilio at Longega	1	0	20	34	11	0	34
6	Casies at Colle	0	0	37	43	0	0	20
7	Rienza at Monguelfo	1	0	19	51	6	0	23
8	Anterselva at Bagni	0	0	27	40	1	0	32
9	Plan at Plan	0	0	41	3	0	6	50
10	Passirio at Saltusio	0	0	43	24	3	2	28
11	Ridanna at Vipiteno	0	0	44	26	3	5	22
12	Posina at Stancari	0	0	22	3	71	0	4
13	Cordevole at Saviner	0	0	43	32	10	0	15
14	Cordevole at Vizza	0	0	66	1	0	0	33

Table 3
Permeability index.

Catchment number	Station name	Prevailing rock type	Permeability index
1	Aurino at Cadipietra	Gneiss	1 – Low permeability
2	Aurino at San Giorgio	Gneiss	1 – Low permeability
3	Riva at Seghe	Gneiss	1 – Low permeability
4	Gadera at Mantana	Phyllites; limestones and dolostones	3 – High permeability
5	San Vigilio at Longega	Limestones and dolostones	3 – High permeability
6	Casies at Colle	Gneiss	2 – Intermediate permeability
7	Rienza at Monguelfo	Limestones and dolostones	3 – High permeability
8	Anterselva at Bagni	Gneiss	2 – Intermediate permeability
9	Plan at Plan	Gneiss	1 – Low permeability
10	Passirio at Saltusio	Gneiss	1 – Low permeability
11	Ridanna at Vipiteno	Gneiss	1 – Low permeability
12	Posina at Stancari	Saccharoidal, stratified and massif dolostones	1 – Low permeability
13	Cordevole at Saviner	Sandstones, argillites, biocalcarenites	2 – Intermediate permeability
14	Cordevole at Vizza	Sandstones, argillites, biocalcarenites	2 – Intermediate permeability

precipitation and temperature available for each catchment ranges from 10 to 15 years.

We used a combination of three different approaches to calculate runoff coefficients and initial catchment soil moisture conditions. A continuous soil moisture accounting model was applied to each catchment to trace the soil moisture conditions of catchments in a continuous way and to estimate event water input to catchments in the forms of rainfall, snowfall and snowmelt. Observed runoff was then separated into baseflow and direct flow, and flood events were identified. At the scale of each flood event, a simple event rainfall–runoff model was fitted to the direct hydrograph, following Merz and Blöschl (2009). In this runoff model, the runoff coefficient appears explicitly as a model parameter and can hence be estimated by optimising an objective function. This procedure is less sensitive to the choice of the start and end points of the events than the usual ratio of volumes (Merz and Blöschl, 2009).

The baseflow separation method, the event separation method, the estimation of the runoff coefficient and the continuous soil moisture accounting model are described in the following sections.

The baseflow separation method

The baseflow separation is carried out by means of an automatic method which applies simple smoothing and separation rules to the total streamflow hydrograph (Institute of Hydrology, 1980; Nathan and McMahan, 1990). The basis of the technique may be described as follows. First the minima of 5-day nonoverlapping periods are found for the entire period of record. Next, the time series of the minima is searched for values that are less than 1.11 times the two outer values; such central values are defined as turning points. The baseflow hydrograph is then constructed by simply connecting all the turning points.

Fig. 4 shows the application of this technique to three different catchments for the same period (26 June–6 August 1997, characterised by several short-duration storms) to three different catchments with similar drainage area (catchment 5, 13 and 12). Rainfall input in catchment 5 produces a slow increase in baseflow, until a certain threshold is reached. When this threshold is exceeded (with the storm of 28th of July), the catchment generates direct runoff. This behaviour is clearly due to the large groundwater storage (largely karstified) characterising this catchment. Production of direct runoff volumes is both more continuous and important for catchments 13 (Cordevole at Saviner) and 12 (Posina at Stancari). Fig. 4 shows that the baseflow separation technique corresponds to what one would separate manually by visual inspection for three very different baseflow behaviours.

The event separation method

The event separation method, which is based on the methodology used by Merz and Blöschl (2009), consists of three steps: (i) screening of peak flows to identify potential event peak flows; (ii) determination of starting time for each event; and (iii) determination of the time corresponding to the end of the event.

For a peak flow to be the peak flow of a flood event, two conditions need to be met: (i) the ratio of direct runoff to baseflow at the peak time needs to be larger than 0.5 (for catchment 5 this threshold was set to 0.2 due to the particularly weak hydrological response); and (ii) there do not exist larger flow in the previous and following 12 h.

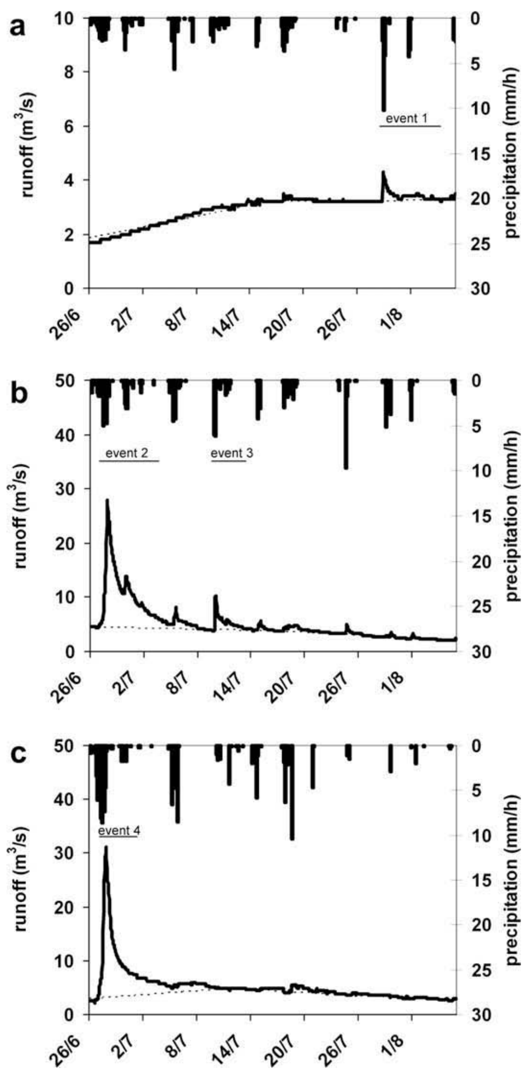

Fig. 4. Separation of baseflow and runoff events for the period (26 June–6 August 1997) for (a) catchment 5 (San Vigilio at Longega), (b) catchment 13 (Cordevole at Saviner) and (c) catchment 12 (Posina at Stancari).

The determination of the start and end points of each event follows an iterative procedure and requires the estimation of a characteristic time scale t'_c, computed according to Merz and Blöschl (2009). The parameters of the iterative procedure are η_j and ε_j. For each peak flow, the start of an event is searched backwards from t_p to $t_p - \eta \cdot t'_c$. The start of an event was assumed to be that time t_s for which

$$q^d(t_s) < \varepsilon_j \cdot q^d(t_p) \tag{1}$$

where $q^d(t_s)$ is the direct runoff at time t_s and $q^d(t_p)$ is the direct runoff at time of peak t_p, i.e. the time where the direct runoff becomes small compared to the direct runoff at the time of the flow peak. If no starting point is found, the search is repeated and η_j and ε_j are gradually increased in five iterations (j = 1–5) to η_j = 0.5; 1.0; 1.5; 2.0; 2.5 and ε_j = 0.01; 0.03; 0.1; 0.2; 0.4, respectively. With this iterative approach, the direct runoff at the beginning of an event is as small as possible but if no such point in time is found, a higher direct runoff is allowed.

In a similar fashion, the time t_e of the end of each event is identified by searching in the time window between t_p and $t_p + 4\eta_j \cdot t'_c$.

All potential events for which the beginning and end points could be identified, for which the peak flow at time t_p is larger than any other discharge within the event, and for which $t_p - t_s > 3h$ and $t_e - t_p > 6h$, are considered acceptable events.

Estimation of the runoff coefficient

Event runoff coefficients are usually estimated as the ratio of event runoff volume and event rainfall volume. This is straightforward if all events are clearly separated and direct runoff between events is small. However, if the direct runoff at the end of an event is significantly larger than zero this ratio will underestimate the runoff coefficient as the trailing limb of the hydrograph is trimmed. To overcome this problem we fitted a simple event rainfall–runoff model to the direct hydrograph. In this runoff model, the runoff coefficient appears explicitly as a model parameter and can hence be estimated by optimising an objective function.

The model is composed by a linear storage with storage parameter k_d and a constant runoff coefficient r_c. The direct runoff over the time period $t_s - t_e$ was simulated with catchment rainfall plus snowmelt inputs (as computed based on the water balance model described below) over the time period $t_s - t'_c/10$ to $t_e - t'_c/10$. The Shuffled Complex Evolution optimisation scheme (Duan et al., 1992) was used to calibrate the two model parameters minimising the root mean square difference between the observed direct runoff hydrograph and the simulated direct runoff hydrograph. The parameter r_c was allowed to range between 0 and 1 while k_d was allowed to range between $0.5t'_c$ and $40t'_c$.

In this study only the runoff coefficients for which the root mean square error of the fitting was less than 70% of the average direct runoff were considered. Moreover, with the aim of selecting the more important events, we retained for each catchment the largest 3N events that passed the statistical analysis, where N is the number of years of recorded data. Following this procedure, the runoff coefficient for a total of 535 events was computed.

The continuous soil moisture accounting hydrological model

The continuous hydrological model used in this paper is a semi-distributed conceptual rainfall–runoff model (Borga, 2002; Borga et al., 2006; Norbiato et al., 2008). The model is used in this study to estimate the initial soil moisture conditions at the start of each runoff event, to discriminate between solid and liquid precipitation during events (solid precipitation during an event will not directly contribute to event runoff) and to estimate snow melt from an existing snow pack which will add to any liquid precipitation.

The model runs on a hourly time step and consists of a snow routine, a soil moisture routine and a flow routing routine. The snow routine represents snow accumulation and melt by using a distribution function approach based on a combined radiation index degree–day concept (Cazorzi and Dalla Fontana, 1996). Catch deficit of the precipitation gauges during snowfall is corrected by a snowfall correction factor (SCF). A threshold temperature interval is used to distinguish between rainfall, snowfall and a mix of rain and snow.

Potential evapotranspiration is estimated by using the Hargreaves method (Hargreaves and Samani, 1982).

The soil moisture routine uses a probability distribution to describe the spatial variation of water storage capacity across a basin. Saturation excess runoff generated at any point in the basin is integrated over the basin to give the total direct runoff entering the fast response pathways to the basin outlet. Drainage from the soil enters slow response pathways. Storage representations of the fast and slow response pathways yield a fast and slow response at the basin outlet which, when summed, gives the total basin flow. The probability distributed moisture (PDM) model configuration used here employs a Pareto distribution of storage capacity, c (Moore, 1985). This has the distribution function

$$F(c) = 1 - [1 - (c/c_{\max})]^b \quad (2)$$

where $c_{\max}$ is the maximum storage capacity in the basin and the parameter b controls the degree of spatial variability of storage capacity over the basin. The instantaneous rate of fast runoff generation from the basin is obtained by multiplying the rainfall rate by the proportion of the basin which is saturated. Saturation excess runoff generated at any point in the basin is integrated over the basin to give the total direct runoff entering the fast response pathways to the basin outlet. Drainage from the soil enters slow response pathways. Storage representations of the fast and slow response pathways yield a fast and slow response at the basin outlet which, when summed, gives the total basin flow.

Losses due to evapotranspiration are calculated as a function of potential evapotranspiration and the status of the soil moisture store. Drainage to the slow flow path is represented by a function of basin moisture storage and the slow or base flow component of the total runoff is assumed to be routed through an exponential store. Direct runoff from the proportion of the basin where storage capacity has been exceeded is routed by means of a geomorphology-based distributed unit hydrograph (Da Ros and Borga, 1997). For model application, the topography is represented by using digital elevation model (DEM) data at three different resolutions: 25 m for catchments 13 and 14, 20 m for catchment 12, 30 m for catchments 1–11.

The Shuffled Complex Evolution optimisation method (Duan et al., 1992) was used in combination with manual calibration to estimate the hydrological model parameters over the 14 catchments. Table 4 shows the period with data available for model calibration and validation. In an effort to improve the description of soil moisture conditions before the flood events we placed equal weight to the representation of low flows and floods.

The following objective functions were used during the optimisation process for this study:

1. the Nash and Sutcliffe (1970) coefficient of efficiency defined as:

$$E_{\mathrm{NS}} = 1 - \frac{\sum_{i=1}^{n}(O_i - S_i)^2}{\sum_{i=1}^{n}(O_i - O_{\mathrm{ave}})^2} \quad (3)$$

where O_i is the hourly ith observed discharge, S_i is the simulated discharge, O_{ave} is the mean value of the observed discharges and n is the number of hourly values in the calibration data set. The coefficient of Efficiency was selected because it is dimensionless and is easily interpreted. If the model predicts observed streamflow with perfection then $E_{\mathrm{NS}} = 1$. If $E_{\mathrm{NS}} < 0$ then the model's predictive power is worse than simply using the average of the observed values.

2. the relative bias (RB) defined as:

$$\mathrm{RB} = \frac{\sum_{i=1}^{n}(S_i - O_i)}{\sum_{i=1}^{n}O_i} \quad (4)$$

RB is a measure of total volume difference between observed and simulated streamflows. Positive RB indicates overestimation of runoff, negative RB indicates underestimation of runoff.

A simple split sample test (Klemes, 1986) was used by dividing the available data into two sets, one used for parameter estimation (calibration period) and the other for model validation (validation period).

Efficiency values for calibration are always larger than 0.5 and the overall Efficiency is around 0.70. When moving from calibration to validation, the overall Efficiency decreases to 0.65 with catchment 4 (Gadera at Mantana) displaying the worst performance ($E_{\mathrm{NS}} = 0.4$). This may be due to the effect of the karstified aquifer, which influences a portion of this catchment. Hydrological response changes widely across this basin in relation to its local geological characteristics, and this enhances the difficulties with the simulation by a lumped model. Estimation of snow accumulation in high altitude catchments, and in particular the temporal variability of the SCF parameter, adds to the difficulties related to the geological heterogeneity of the study basins and limits the accuracy of the water balance model.

The overall Efficiency over the whole simulation period is 0.68 with 40% of the catchments characterised by efficiencies greater than 0.7. Bias values for calibration and validation range between −5% and 11%.

Fig. 5 shows one year of simulation results for catchment 14 (Cordevole at Vizza). Fig. 5a shows that for this catchment the implemented modelling approach yields hydrologically acceptable representations of the watershed behaviour. At this scale, the simulated and observed hydrographs appear visually similar. Fig. 5b shows that high and low residuals are homogeneously distributed over the year with a maximum value occurring during the September flood. In Fig. 5c the relative soil moisture content of the PDM storage (given in Eq. (2)) has been plotted. This figure shows clearly how soil moisture status increases starting from April, when snowmelt begins, and decreases after October, when snow accumulation starts on the catchment.

Table 4
Periods with data available.

Catchment number	Station name	Periods with hourly data available
1	Aurino at Cadipietra	1/10/89-31/12/2004
2	Aurino at San Giorgio	1/10/89-31/12/2004
3	Riva at Seghe	1/10/89-31/12/2004
4	Gadera at Mantana	1/10/89-31/12/2004
5	San Vigilio at Longega	1/10/89-30/09/97 1/10/2002-31/12/2004
6	Casies at Colle	1/10/89-31/12/2004
7	Rienza at Monguelfo	1/10/89-31/12/2004
8	Anterselva at Bagni	1/10/89-31/12/2004
9	Plan at Plan	1/10/94-31/12/1997 1/10/2002-31/12/2004
10	Passirio at Saltusio	1/10/94-31/12/2004
11	Ridanna at Vipiteno	1/10/89-31/12/2004
12	Posina at Stancari	1/10/92-31/12/1999
13	Cordevole at Saviner	1/10/92-31/12/2003
14	Cordevole at Vizza	1/10/92-31/12/2003

Results

The cumulative distribution functions of the event runoff coefficients for the study catchments are shown in Fig. 6 while the corresponding summary statistics are reported in Table 5. Table 5 shows that the mean runoff coefficients range more than one order of magnitude, from 0.04 (catchment 5) to 0.48 (catchment 12). This points to the large variability of the hydrological response in the study area. Interestingly, catchment 5 and catchment 12 are, respectively, the driest and the wettest catchments in the study set. Both the coefficient of variation and the skewness of the distributions decrease with an increase of the mean value, as shown in Fig. 7a and b. These results are consistent with those reported by Merz and Blöschl (2009). Catchments with high mean runoff coefficients are characterised by distribution functions that are almost uniform. Conversely, catchments with low mean runoff coefficients exhibit often highly skewed distribution functions and large outliers. This reflects the occurrence of locally rare large runoff events

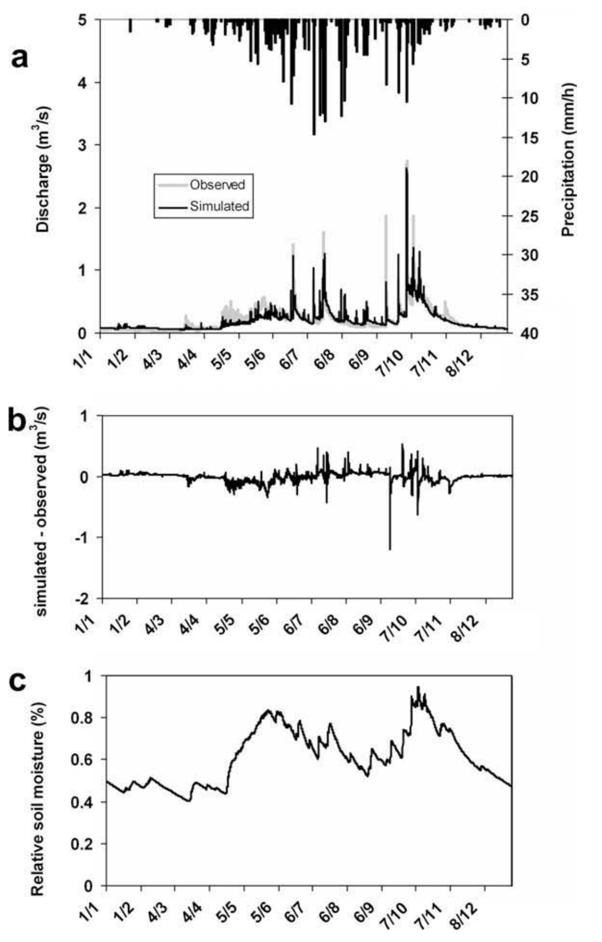

Fig. 5. One year (01.01.1993–31.12.1993) of hourly results from the water balance PDM model for the Cordevole river at Vizza (a) simulation results, (b) simulation residuals and (c) relative soil moisture content of the PDM storage.

even in catchments with low mean runoff coefficients, resulting in highly skewed distributions.

The overall mean value of the runoff coefficient is 0.28, whereas the mean coefficient of variation is 0.57 and mean skewness is 1.18. These values are intermediate between those reported by Merz and Blöschl (2009), who reported 0.4 and 0.84 for the mean and the skewness, respectively, for their alpine region, and Gottschalk and Weingartner (1998), who reported a mean value of 0.1 for their alpine region and 0.19 for their southern alpine region. Reasons for this may be found when examining the physical characteristics of the study catchments. Snow and glacier melt has an important role on distribution of runoff coefficients in the alpine catchments analysed by Merz and Blöschl (2009), by increasing the antecedent soil moisture through snow and ice melt. This effect, which increases the value of the runoff coefficients, is likely to be less important in our study. Differences may also due to the use of different procedures for the computation of the event runoff coefficient, which may give rise to different results, as shown by Blume et al. (2007).

Results from this analysis are reported with more detail for three catchments with similar drainage areas (catchment 5, 12 and 13, with areas ranging from 105 to 116 km^2) (Fig. 8a–c), but vastly differing hydrologic response. Catchment 5 (San Vigilio at Longega) and 12 (Posina at Stancari) represent two end members as far as the runoff coefficients distribution is concerned, as mentioned above, whereas catchment 13 (Cordevole at Saviner) has intermediate response.

On the left panel, direct runoff depths have been plotted against the event precipitation depths, showing the large variability of the climatic forcing, with maximum estimated event precipitation of up to 100 mm in the San Vigilio to 420 mm in the Posina. Examination of this panel shows also that dependence of runoff depths on rainfall depths increases when moving from San Vigilio to the Posina. Examination of the central panel, where runoff coefficients are plotted against corresponding runoff depths, shows that the runoff coefficients increase with increasing runoff depths, as expected, implying the strong nonlinearity of the rainfall–runoff process (Sivapalan et al., 2002). However, it is interesting to note that the runoff coefficients of San Vigilio vary in a relatively small range until a runoff threshold is exceeded, after which they show a sudden increase.

While this behaviour is expected in catchments influenced by a large groundwater storage (and in particular on karstified catchments, Phillips, 2006), this provides also an explanation for the large outliers reported for this catchment. On the right panel, event discharge peaks have been plotted against the corresponding runoff depths to provide insight into how the shape of the hydrograph varies with runoff volume (Michaud and Sorooshian, 1994). Examination of this panel shows that the linearity of the relationship between peak discharges and runoff depths increases when moving

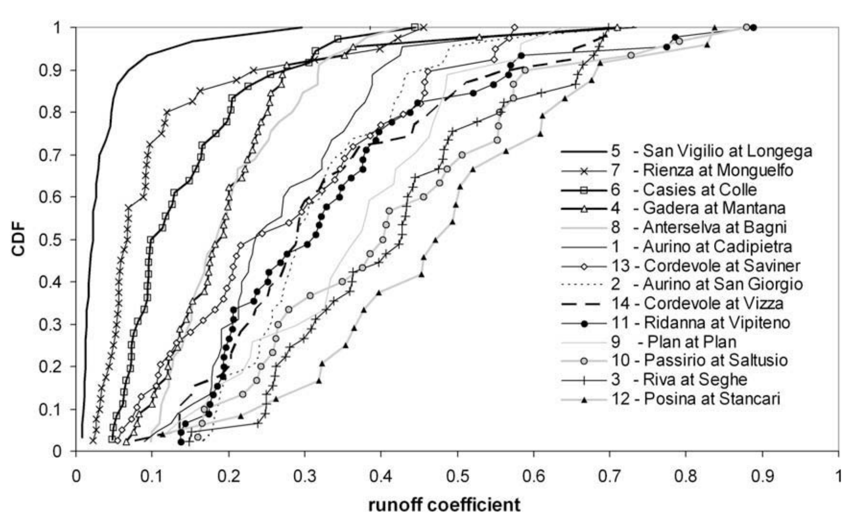

Fig. 6. Distribution function of the event runoff coefficients for the study catchments.

Table 5
Sample moments of the event runoff coefficients.

Catchment number	Station name	Number of events	Mean	CV	Skewness
1	Aurino at Cadipietra	45	0.28	0.43	1.4
2	Aurino at San Giorgio	45	0.32	0.38	1.13
3	Riva at Seghe	45	0.42	0.36	0.30
4	Gadera at Mantana	45	0.20	0.55	2.45
5	San Vigilio at Longega	30	0.04	1.50	3.59
6	Casies at Colle	36	0.14	0.64	1.49
7	Rienza at Monguelfo	40	0.11	1.00	2.12
8	Anterselva at Bagni	45	0.21	0.38	0.82
9	Plan at Plan	27	0.37	0.38	−0.03
10	Passirio at Saltusio	30	0.42	0.45	0.62
11	Ridanna at Vipiteno	45	0.34	0.53	1.34
12	Posina at Stancari	24	0.48	0.38	0.13
13	Cordevole at Saviner	39	0.28	0.57	0.37
14	Cordevole at Vizza	39	0.33	0.48	0.85

from the San Vigilio to the Posina. This agrees with the flashy character of the Posina runoff response, which contrasts with the delayed and multipeaked response of the San Vigilio, where runoff is generated only during long-lasting rainfall events.

It is now interesting to see whether the large variability and the patterns emerging from this analysis can be explained in terms of hydrological, climatological, geological and land use properties. These controls are evaluated in the following sections.

The role of climate

Climate variability strongly impacts upon the mechanisms of flood generation in two ways: in a direct way through the variability of storm characteristics and indirectly through the seasonality of rainfall and evapotranspiration which then affect the antecedent catchment conditions for individual storm events (Sivapalan et al., 2005). Mean areal precipitation (MAP) is used here to describe the

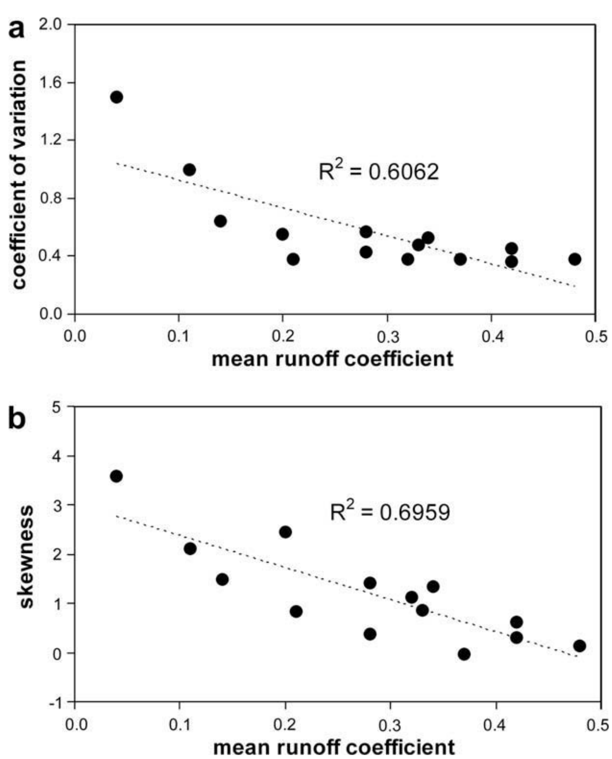

Fig. 7. Mean runoff coefficients plotted vs.: (a) coefficients of variation of runoff coefficients, and (b)skewness of runoff coefficients.

climate variability across the catchments. Fig. 9a shows that mean event rainfall generally increases with MAP (even though in a non-linear way) across the study catchments. This shows that MAP can be used as a surrogate, at least partially, of the characteristics of storm events leading to floods. Catchment mean runoff coefficients are plotted against MAP in Fig. 9b. This figure shows that a significant linear relationship may be found between these two variables for the study catchments ($R^2 = 0.83$; least squares linear regression is significant at the 1% level). The significance of this relationship means that MAP influences the distribution of runoff coefficients not only through the characteristics of the flood-generating storm events, but also by controlling the variability of the initial conditions. For instance, by increasing MAP, it becomes more likely that initial conditions are wet, thus enhancing runoff generation. This means also that with increasing MAP, the probability of having outliers of runoff coefficients is less, leading to distribution functions that are less skewed. At longer time scales, MAP may influence the distribution of runoff coefficient by controlling the geomorphological structure of catchments, through soil formation and erosion processes, as exemplified by the positive relationship between drainage density and MAP (Melton, 1957; Gregory and Gardiner, 1975; Gregory, 1976).

The results reported in this Section agree with those obtained by Merz and Blöschl (2009), who also found that MAP is an important control on the statistical characteristics of the runoff coefficients, and that mean event runoff coefficient increases by increasing MAP.

The role of geology

Given the significant control exerted by MAP on the runoff coefficient distribution, the role of geology has been assessed taking into account the influence of MAP. In Fig. 10 the mean runoff coefficients have been plotted against MAP by using different grey gradation to signify variation of the permeability index (Table 3). Fig. 10 shows that the mean runoff coefficient increases with permeability ranking (from high permeability to low permeability), as expected. It is important to note that the most (less) permeable catchments happen also to be those characterised by low (high) MAP. This is an important non-physical feature of the sampling structure of our study that needs to be accounted for in the analysis. Since the two controls act in the same way, the influence of geology on runoff coefficients can be isolated only by comparing catchments with similar MAP. This is the case for the Catchments 4–8, 13 and 14, with MAP ranging between 900 and 1200 mm. For these catchments, the runoff coefficient increases with decreasing permeability, as expected, with the exception of Catchments 4 and 6. For these last catchments, the geological classification may be not completely representative of the local geological complexity. Less permeable catchments have larger runoff coefficients, as expected, but our data and the geological classification considered here cannot be used to isolate the individual effect of geology and climate in these cases. A counteractive situation is found for Catchments 1 and 13, where catchment 1 has lower permeability and higher MAP than catchment 13. In spite of these characteristics, which would suggest a higher runoff coefficient for catchment 1 with respect to catchment 13, the mean observed runoff coefficient is the same (even though the cumulative distribution is rather different, Fig. 6).

The role of soil types and land cover

There is a rich literature on land use change effects on runoff generation during flood events, including Jones (2000), Bronstert et al. (2002), Robinson et al. (2003), Andreassian (2004) and Bloeschl et al. (2007). However, probably the most widely used

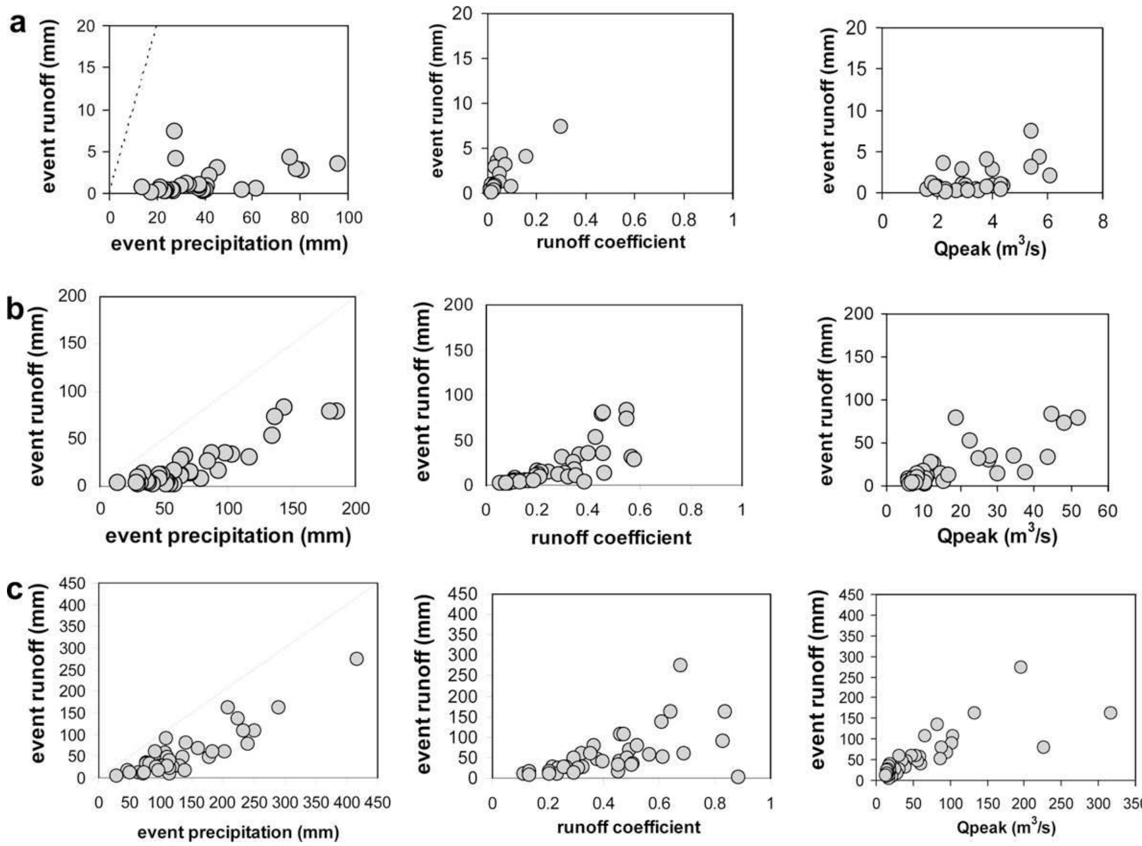

Fig. 8. Event runoff depth vs. event precipitation depth; event runoff depth vs. runoff coefficient; event runoff depth vs. flood peak, for three representative catchments: (a) catchment 5 (San Vigilio at Longega); (b) catchment 13 (Cordevole at Saviner); and (c) catchment 12 (Posina at Stancari). Note the change of scale for the three catchments.

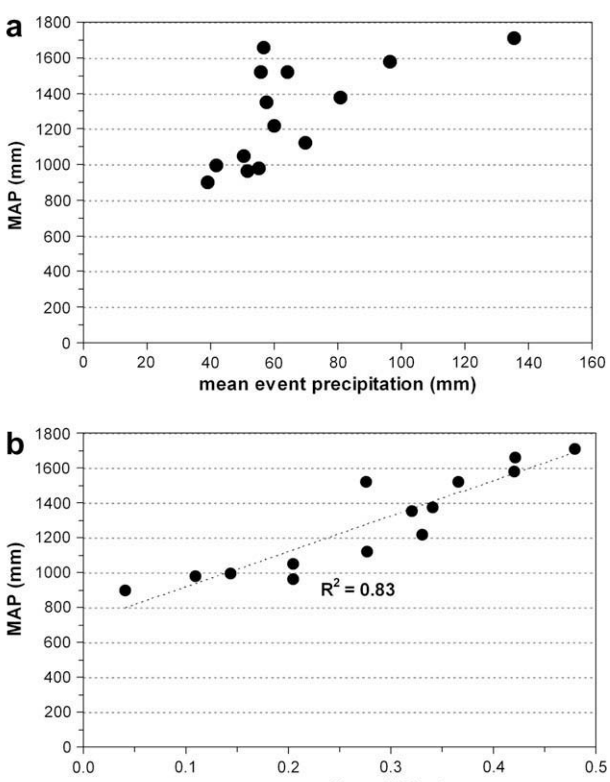

Fig. 9. Mean annual precipitation (MAP) plotted vs.: (a) mean event precipitation; and (b) mean runoff coefficients, for the study catchments.

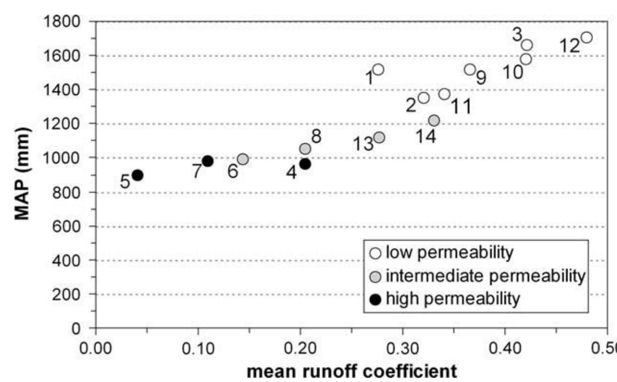

Fig. 10. Mean runoff coefficients vs. mean annual precipitation (MAP) for the study catchments stratified by permeability index.

procedure to index the effects of soils and land use on runoff coefficient is the US-SCS curve number method (US-SCS, 1972; Ponce and Hawkins, 1996). The SCS method provides a procedure for estimating the curve number from soil type and land use and antecedent rainfall. Once the curve number is known it can be used to estimate event runoff depth from event rainfall depth for an ungauged catchment.

In this study we used the SCS curve number to isolate the potential effect of soil and land use variability on event runoff coefficient distribution. The SCS curve number was computed from soil and land use data. The soil map was reclassified to obtain a soil group map (US-SCS, 1972) which, combined with the land use map, yielded a curve number map. Finally, the average curve number was computed for every catchment. Since the curve number is used here as an index of the mean catchment response, antecedent rainfall conditions are assumed to be average for all catchments. For every catchment, Fig. 11 shows the 90%, 50% and 10% quantiles of the runoff coefficient distribution functions against the catchment average curve numbers. The highest curve numbers would be expected to be associated with the highest runoff coefficients. However, this is not fully borne out in the results reported in Fig. 11. For instance, the smallest value of curve number is reported for catchment 12 (Posina at Stancari), which is characterised by the largest runoff coefficient. Land use in catchment 12, in fact, is dominated by forests. Consequently the SCS method predicts relatively small values of the curve number, as forest soils are usually highly permeable. However, in this catchment soil permeability seems to have relatively little effect on the runoff coefficients with respect to storm event and climatic characteristics. On the other hand, catchments 4, 5, 7 and 10, whose mean runoff coefficients span almost the complete range of computed runoff coefficients, are characterised by very similar values of the curve number.

These results shows that land use effects on the runoff coefficients, as indexed by the SCS-CN method, is outweighed by climatic and geologic effects. Among other things, this may be related to the way rock outcrops have been considered in the computation of the curve number. With this method, rock outcrops are generally associated with almost impervious surfaces and hence high curve numbers. However, insight obtained from site visits as well as previous results on the role of geology have shown that runoff generation from rock outcrops depends heavily on the lithological units, with rainfall being completely and fastly drained in karstified limestones and through faults and fissures of limestones and dolomites (such as those present in the San Vigilio catchment).

The role of initial soil moisture conditions

Evaluation of the role of initial soil moisture conditions on the distribution of event runoff coefficients requires consideration of two factors: subsurface water storage capacity and initial wetness status. The rationale for the selection of these factors is that the impact of antecedent moisture conditions is expected to increase with increasing subsurface water storage capacity. In this study, the catchment subsurface water storage capacity is indexed based on the standardised flow–duration curve (i.e. expressed as a percentage of the mean flow). In this way, the dependencies of the index on the climatic variability and on the scale effect of catchment area are minimised. The shape of the standardised flow–duration curve reflects the characteristic response of a catchment to rainfall. The gradients of the log-transformed standardised flow–duration curves for a range of catchments with differing geology (Fig. 12) illustrate that low permeability catchments have high gradient curves reflecting a very variable flow regime; low storage of water in the catchment results in a quick response to rainfall and small low flows in the absence of rainfall. Low gradient flow–duration curves indicate that the variance of daily flows is low, because of the damping effects of groundwater storages provided naturally, for example, by extensive karstified or limestone aquifers. The ratio of daily discharge which is exceeded 90% of the time to the median daily flow, Q_{90}/Q_{50}, has hence been used as an index of subsurface water storage capacity (Borga et al., 2007).

Values of the subsurface water storage capacity index (Q_{90}/Q_{50}) are reported for each catchment in Table 6, which shows also the permeability index. In general there is a good correspondence between the permeability index and the subsurface water storage capacity index, with the latter increasing with the permeability ranking. An exception is catchment 13, and, to a lesser degree, catchment 8. Even though catchments 13 and 14 have similar geologic classification (catchment 14 is nested in the larger parent catchment 13), Table 6 suggests that it is likely that the permeability of catchment 14 is lower than the one derived from the geologic classification.

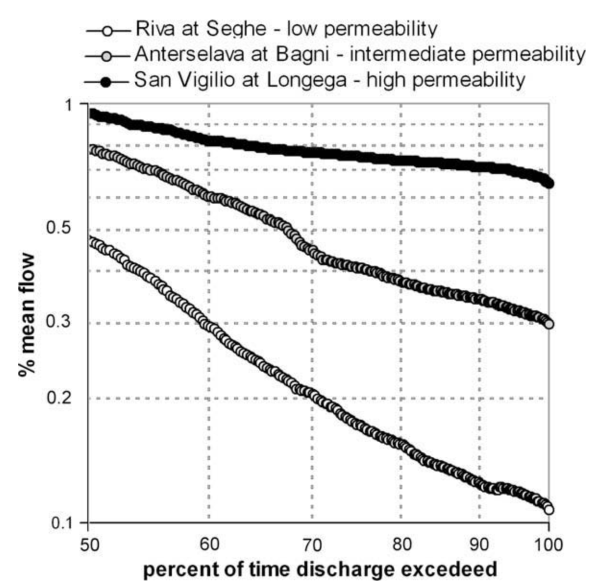

Fig. 12. The influence of geology on the gradient of the standardised flow–duration curve.

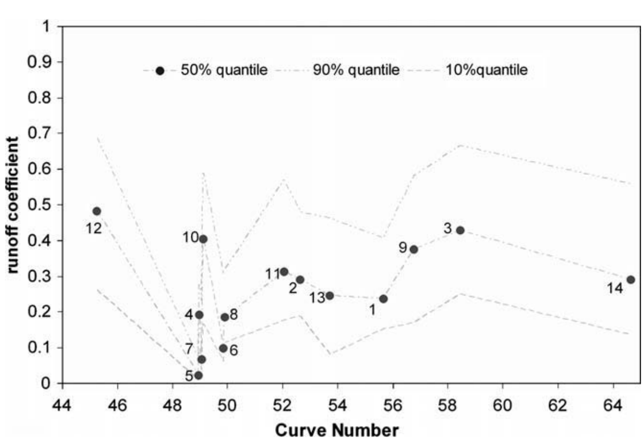

Fig. 11. Quantiles of the runoff coefficient distributions vs. the SCS curve number.

Table 6
The soil moisture capacity index (Q_{90}/Q_{50}). The table reports also the permeability index. (1 = low permeability, 3 = high permeability).

Catchment number	Station name	Q_{90}/Q_{50}	Permeability index
3	Riva at Seghe	0.26	1
14	Cordevole at Vizza	0.30	2
9	Plan at Plan	0.33	1
11	Ridanna at Vipiteno	0.39	1
1	Aurino at Cadipietra	0.41	1
10	Passirio at Saltusio	0.44	1
8	Anterselva at Bagni	0.44	2
12	Posina at Stancari	0.45	1
2	Aurino at San Giorgio	0.47	1
13	Cordevole at Saviner	0.51	2
6	Casies at Colle	0.52	2
7	Rienza at Monguelfo	0.58	3
4	Gadera at Mantana	0.58	3
5	San Vigilio at Longega	0.75	3

The initial soil moisture conditions have been derived by examining the simulated relative soil moisture content of the PDM storage. Relative initial soil moisture conditions larger than the median value of the initial soil moisture distribution functions were considered "wet", while lower values were considered "dry". This allowed us to split the flood events into two classes termed "wet" and "dry", according to the corresponding initial soil moisture conditions. Moreover, in order to isolate the effect of initial conditions with respect to the effect of rainfall depth, we considered only the catchments for which the distributions of event rainfall depths following dry and wet periods were similar. In these catchments, the

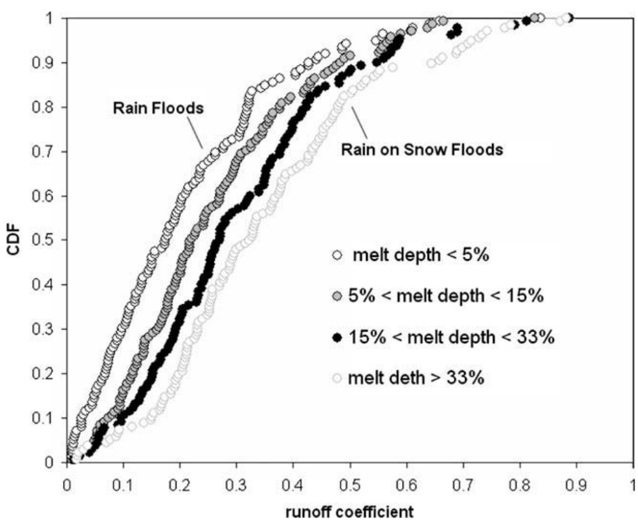

Fig. 13. Distribution function of the event runoff coefficients for all the catchments stratified by the percentage of snow melt over event precipitation depth.

probability of having high or low rainfall depths is expected to be the same both following dry and wet periods. This led to exclude five catchments (2, 6, 8, 10 and 14) from the analysis. As a final step, to isolate the effect of initial soil moisture conditions, we considered the events less influenced by initial snowcover and snowmelt. Fig. 13 shows the distribution functions of the runoff coefficients classified by different ranges of the snowmelt volumes over total precipitation ratio. The runoff coefficients increase when the contribution of melt increases, in agreement with findings by Merz and Blöschl (2009). In this analysis we considered the events with snow melt depths of less than 33% of the event precipitation depth. These events represent 70% of the total events.

The role of the initial soil moisture conditions has been examined by contrasting the distribution function of the runoff coefficients for 'wet' events with respect to the distribution of the 'dry' events. This analysis is reported with some details in Fig. 14 for three representative catchments: catchment 5 (San Vigilio at Longega), catchment 13 (Cordevole at Saviner) and catchment 3 (Riva at Seghe). Catchments 5 and 3 represent two end members as far as the subsurface water storage capacity index is concerned, with index values of 0.75 and 0.26, respectively. Catchment 13 has an intermediate index value, amounting to 0.51. Fig. 14 shows the distribution function of the initial relative soil moisture (left panel), the distribution functions of event precipitation for 'dry' and 'wet' events (central panel) and the distribution functions of the event runoff coefficients for 'dry' and 'wet' events (right panel). The central panel shows that the distributions of precipitation depths during dry and wet periods are similar, as expected after the design of the analysis. The right panel shows that the distribution of 'wet' runoff coefficients differs with respect to the 'dry' one (with a shift towards higher values of runoff coefficient) only for the intermediate catchment 13. In the other two cases, the two distributions almost overlap. This behaviour is expected for catch-

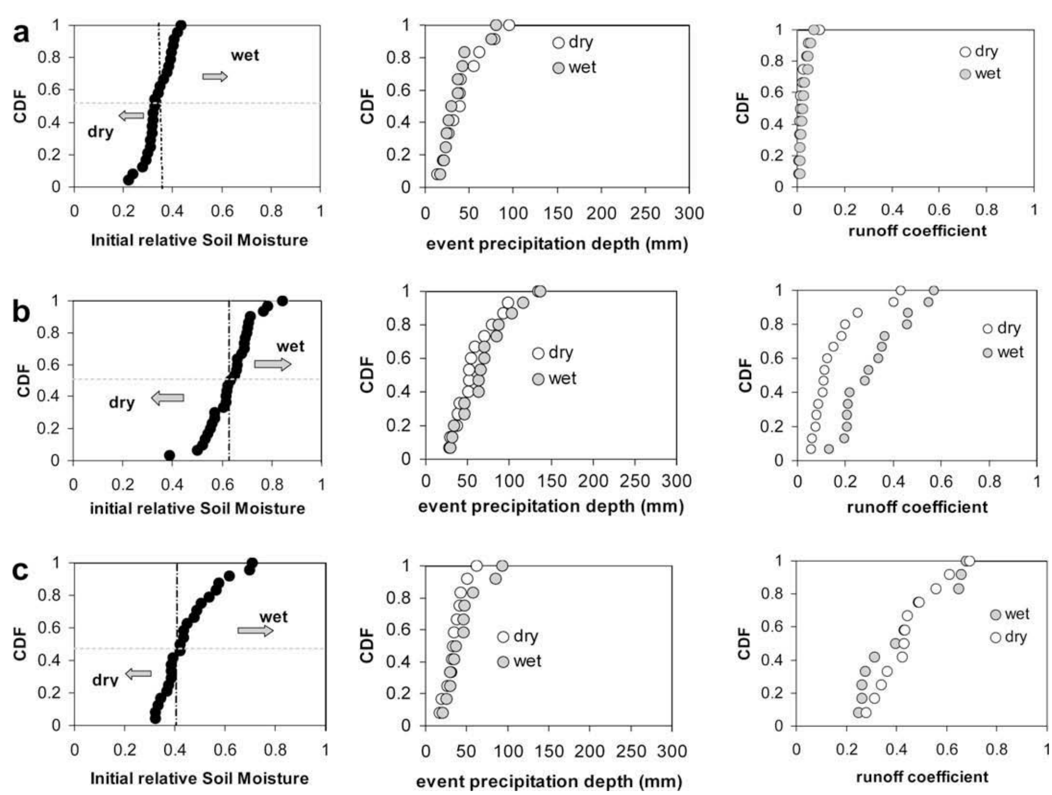

Fig. 14. Distribution functions of initial relative soil moisture, event precipitation depths and runoff coefficients for dry and wet periods (a) catchment 5 (San Vigilio at Longega), (b) catchment 13 (Cordevole at Saviner), and (c) catchment 3 (Riva at Seghe).

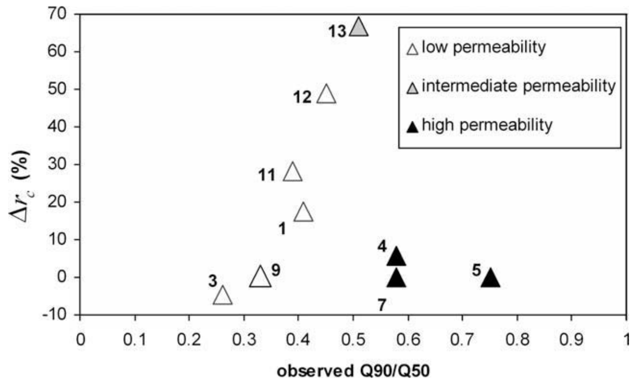

Fig. 15. Relative difference between 'wet' and 'dry' runoff coefficients vs. subsurface water storage capacity, as indexed by the parameter Q_{90}/Q_{50}.

ment 3; in this case, the low subsurface water storage capacity minimises the effect of initial soil moisture conditions. However, it is not expected for catchment 5, characterised by high values of the subsurface water storage capacity index. To evaluate these aspects, we have computed the relative difference between the mean values of the distributions of 'wet' and 'dry' runoff coefficients for the catchments considered, as follows:

$$\Delta r_c = \frac{r_{c,\mathrm{wet}_{\mathrm{mean}}} - r_{c,\mathrm{dry}_{\mathrm{mean}}}}{r_{c_{\mathrm{mean}}}} \tag{5}$$

The relative difference of the mean values (termed 'relative difference' hereafter) is reported in Fig. 15 together with the corresponding subsurface water storage capacity index. This figure shows that the influence of the initial soil moisture conditions does not increase with the subsurface water storage capacity. Actually, there exists an intermediate region of subsurface water storage capacity, as indexed by the capacity index, which maximises the impact of initial soil moisture conditions on the runoff coefficient. According to this study, this intermediate region ranges between index values of 0.35 and 0.55. For catchments with larger index values (such as catchments 4, 7 and 5) the difference between mean values of 'wet' and 'dry' runoff coefficients is negligible. In these catchments, characterised by large subsurface water storage capacity (represented, for instance, by a karstified aquifer), the soil moisture storage is more quickly connected to the groundwater storage and the initial available capacity is generally larger than event precipitation, even in 'wet' conditions. In these cases, runoff is generated on relatively small portions of the catchment which are not intercepted by the karstified aquifer. On the other hand, in low permeability catchments, runoff response is always relatively large (and catchment memory is shorter), so the effect of initial soil moisture is small.

Conclusions

There are five principal observations from our work.

1. The large spatial variability in mean runoff coefficient, which ranges from 0.04 to 0.48, is relatively well explained by mean annual precipitation. Runoff coefficients tend to increase with mean annual precipitation. The significance of this relationship means that mean annual precipitation influences the distribution of runoff coefficients not only through the characteristics of the flood-generating storm events, but also by controlling the variability of the initial conditions and, at longer time scales, likely by controlling the geomorphological structure of catchments, through soil formation and erosion processes. The coefficient of variation and skewness of the runoff coefficients tend to decrease with increasing mean annual precipitation.
2. Geological characteristics (as indexed by the 'permeability index') influence the distribution of the runoff coefficients, at least for mean annual precipitation less than 1200 mm, through their direct effect on hydrologic pathways and storage properties. Catchments characterised by a high permeability index have lower mean runoff coefficients than catchments with low permeability index and similar mean annual precipitation. Less permeable catchments have larger runoff coefficients, as expected. However, our data and the geological classification considered here cannot be used to isolate the individual effect of geology and climate in these last cases, since catchments with low permeability index have also high mean annual precipitation.
3. Land use, as indexed by the SCS curve number, influences the runoff coefficient distribution to a lesser degree. This result may be related to ambiguities in the SCS curve number-based indexing (particularly for rock outcrops) and forests. The small effects of land use and soil types on the event runoff coefficients may also be related to scale. The catchments analysed in this study are medium sized catchments with catchment area ranging from 7.3 to 608.4 km^2. Once one moves to smaller scales, particularly hillslopes, soils and land use clearly become more important as illustrated by numerous plot scale studies (e.g. Kirnbauer et al., 2005).
4. An analysis of the runoff coefficients by flood type indicates that runoff coefficients increase with event snowmelt, and are relatively low for rain floods. The effect of snow processes mainly seems to be in increasing antecedent soil moisture.
5. Results show that there exists an intermediate (most sensitive) region of subsurface water storage capacity, as indexed by a flow–duration curve-based index, which maximises the impact of initial soil moisture conditions on the runoff coefficient. This means that the difference between runoff coefficients characterised by wet and dry initial conditions is negligible both for basins with very large subsurface water storage capacity (mainly due to karstified aquifers) and for basins with small storage capacity. For basins with intermediate storage capacities, the difference (and hence the impact of the initial soil moisture conditions) is relatively large.

Overall, this work can provide the basis for developing a model that is able to predict runoff coefficients for ungauged catchments in the eastern Italian Alps and similar climates and geologies. It shows that a geological framework, including detailed information on the degree of secondary permeability and spatial organisation of the lithological units, provides a useful basis for interpreting the distribution of runoff coefficients in the study area. Although the mountainous landscapes of this region have many distinctive attributes that lend themselves well to this kind of analysis, we maintain that the degree to which geology affects flood regime in this region is not unique. This paper provides an illustrative example that suggests that progress toward resolving the problem of predicting flood response in ungauged basins can be made by explicitly structuring the analysis of streamflow using climatic information and geo-hydrologic landscape types. However, the information about hydrologically-relevant characteristics of the geological formations is only rarely available at the regional scale. Results from this work suggest that a major task within the Predictions in Ungauged Basins initiative may be to characterise these geo-hydrologic landscape types and to evaluate their relationships with flood regimes.

Acknowledgments

This work was supported by the European Community's Sixth Framework Programme through the grant to the budget of the

Integrated Project *FLOODsite*, Contract GOCE-CT-2004-505420 and in part by the STREP Project *HYDRATE*, Contract GOCE 037024. Data for the Adige and Brenta river systems were kindly provided by Provincia Autonoma di Bolzano - Ufficio Idrografico and by Provincia Autonoma di Trento – Servizio Bacini Montani, respectively. ARPA – Regione Veneto kindly provided the data for the Bacchiglione and Piave river systems. The authors would also like to thank the Austrian Academy of Sciences (APART [Austrian Programme for Advanced Research and Technology] –fellowship) and the FWF Project No. P18993-N10 for financial support.

References

Andreassian, V., 2004. Waters and forests: from historical controversy to scientific debate. Journal of Hydrology 291, 1–27.

Blume, T., Zehe, E., Bronstert, A., 2007. Rainfall runoff response, event-based runoff coefficients and hydrograph separation. Hydrological Sciences Journal 52 (5), 843–862.

Borga, M., 2002. Accuracy of radar rainfall estimates for streamflow simulation. Journal of Hydrology 267, 26–39.

Borga, M., Degli Esposti, S., Norbiato, D., 2006. Influence of errors in radar rainfall estimates on hydrological modelling prediction uncertainty. Water Resources Research 42, W08409. doi:10.1029/2005WR004559.

Borga, M., Boscolo, P., Zanon, F., Sangati, M., 2007. Hydrometeorological analysis of the August 29, 2003 flash flood in the eastern Italian Alps. Journal of Hydrometeorology 8 (5), 1049–1067.

Bronstert, A., Niehoff, D., Bürger, G., 2002. Effects of climate and land-use change on storm runoff generation: present knowledge and modelling capabilities. Hydrological Processes 16 (2), 509–529.

Bloeschl, G. et al., 2007. At what scales do climate variability and land cover change impact on flooding and low flows? Hydrological Processes 21, 1241–1247.

Budyko, M.I., 1974. Climate and Life. Academic Press, New York.

Cazorzi, F., Dalla Fontana, G., 1996. Snowmelt modelling by combining air temperature and a distributed radiation index. Journal of Hydrology 181, 169–187.

Cerdan, O., Le Bissonnais, Y., Govers, G., Leconte, V., van Oost, K., Couturier, A., King, C., Dubreuil, N., 2004. Scale effects on runoff from experimental plots to catchments in agricultural areas in Normandy. Journal of hydrology 299, 4–14.

Da Ros, D., Borga, M., 1997. Use of digital elevation model data for the derivation of the geomorphologic instantaneous unit hydrograph. Hydrological Processes 11, 13–33.

Duan, Q., Sorooshian, S., Gupta, S., Gupta, V.K., 1992. Effective and efficient global optimisation for conceptual rainfall–runoff models. Water Resources Research 28 (4), 265–284.

Fiorentino, M., Iacobellis, V., 2001. New insights into the climatic and geologic controls on the probability distribution of floods. Water Resources Research 37 (3), 721–730.

Gottschalk, L., Weingartner, R., 1998. Distribution of peak flow derived from a distribution of rainfall volume and runoff coefficient, and a unit hydrograph. Journal of hydrology 208, 148–162.

Gregory, K.J., 1976. Drainage networks and climate. In: Derbyshire, E. (Ed.), Geomorphology and Climate. John Wiley, New York, pp. 289–315.

Gregory, K.J., Gardiner, V., 1975. Drainage density and climate. Zeitschrift Fur Geomorphologie 19, 287–298.

Hargreaves, G.H., Samani, Z.A., 1982. Estimating potential evapotranspiration. Journal of Irrigation and Drainage Division 108, 225–230.

Institute of Hydrology, 1980. Low Flow Studies Report. Institute of Hydrology,Wallingford, UK.

Jones, J., 2000. Hydrologic processes and peak discharge response to forest removal, regrowth, and roads in 10 small experimental basins, Western Cascades, Oregon. Water Resources Research 36, 2621–2642.

Kirnbauer, R., Blöschl, G., Haas, P., Müller, G., Merz, B., 2005. Identifying space–time patterns of runoff generation: a case study from the Löhnersbach catchment, Austrian Alps. In: Huber, U.M., Bugmann, H.K.M., Reasoner, M.A. (Eds.), Global Change and Mountain Regions – A State of Knowledge Overview. Springer, ISBN 1-4020-3506-3, pp. 309–320.

Klemes, V., 1986. Operational testing of hydrological simulation models. Hydrological Sciences Journal 31, 13–24.

Melton, M. A., 1957. An Analysis of the Relations Among Elements of Climate, Surface Properties, And Geomorphology. Dept. Geol. Columbia Univ. Tech. Rep. 11, Proj. NR 389-042, Off. of Nav. Res., New York.

Merz, R., Blöschl, G., 2003. A process typology of regional floods. Water Resources Research 39 (12), 1340. doi:10.1029/2002WR001952.

Merz, R., Blöschl, G., 2009. A regional analysis of event runoff coefficients with respect to climate and catchment characteristics in Austria. Water Resources Research. doi:10.1029/2008WR007163.

Michaud, J.D., Sorooshian, S., 1994. Comparison of simple vs. complex distributed runoff models on a midsized, semiarid watershed. Water Resources Research 30 (3), 593–605.

Moore, R.J., 1985. The probability-distributed principle and runoff production at point and basin scales. Hydrological Sciences Journal 30, 273–297.

Nash, J.E., Sutcliffe, J.E., 1970. River flow forecasting through conceptual models, part I: a discussion of principles. Journal of Hydrology 10, 282–290.

Nathan, R.J., McMahan, T.A., 1990. Evaluation of automated techniques for baseflow and recession analysis. Water Resources Research 26 (7), 1465–1473.

Norbiato, D., Borga, M., Degli Esposti, S., Gaume, E., Anquetin, S., 2008. Flash flood warning based on rainfall thresholds and soil moisture conditions: An assessment for gauged and ungauged basins. Journal of Hydrology 362 (3-4), 274–290.

Phillips, J.D., 2006. Evolutionary geomorphology: thresholds and nonlinearity in landform response to environmental change. Hydrology and Earth System Sciences 10, 731–742.

Ponce, V.M., Hawkins, R.H., 1996. Runoff curve number: has it reached maturity? Journal of Hydrologic Engineering 1 (1), 11–19.

Robinson, M., Cognard-Plancq, A.-L., Cosandey, C., David, J., Durand, P., Führer, H.-W., Hall, R., Hendriques, M.O., Marc, V., Mccarthy, R., McDonnell, M., Martin, C., Nisbet, T., O'Dea, P., Rodgers, M., Zollner, A., 2003. Studies of the impact of forests on peak flows and baseflows: a European perspective. Forest Ecology and Management 186, 85–97.

Sevruk, B., Paulais, M., Roulet, Y.-A., 1998. Correction of precipitation measurement using fresh snow as reference. In: Proceedings of the WMO Technical Conference on Meteorological and Environmental Instruments and Methods of Observation, TECO-98. WMO/TD-No. 877, Geneva, Switzerland, pp. 349–352.

Sivapalan, M., Takeuchi, K., Franks, S.W., Gupta, V.K., Karambiri, H., Lakshmi, V., Liang, X., McDonnell, J.J., Mendiondo, E.M., O'Connell, P.E., Oki, T., Pomeroy, J.W., Schertzer, D., Uhlenbrook, S., Zehe, E., 2003. IAHS decade on predictions in ungauged basins (PUB), 2003–2012: shaping an exciting future for the hydrological sciences. Hydrological Sciences Journal 48, 857–880.

Sivapalan, M., Jothityangkoon, C., Menabde, M., 2002. Linearity and nonlinearity of basin response as a function of scale: discussion of alternative definitions. Water Resources Research 38 (2), 7–9. doi:10.1029/2001WR000482.

Sivapalan, M., Bloeschl, G., Merz, R., Gutknecht, D., 2005. Linking flood frequency to long-term water balance: incorporating effects of seasonality. Water Resources Research 41, W06012. doi:10.1029/2004WR003439.

Tague, C., Grant, G.E., 2004. A geological framework for interpreting the low-flow regimes of Cascade streams, Willamette River basin, Oregon. Water Resources Research 40, W04303. doi:10.1029/2003WR002629.

US-SCS, 1972. National Engineering Handbook Section 4 Hydrology. US Department of Agriculture.

Van de Griend, A., Seyhan, E., Engelen, G.B., Geirnaert, W., 1986. Hydrological characteristics of an alpine glacial valley in the north Italian Dolomites. Journal of Hydrology 88, 275–299.

Wainwright, J., Parsons, A.J., 2002. The effect of temporal variations in rainfall on scale dependency in runoff coefficients. Water Resources Research 38 (12), 1271.

Winter, T.C., 2001. The concept of hydrologic landscapes. Journal of the American Water Resources Association 37, 335–350.